

Figs. 2 and 3 compare the predictions and experiments of the total excitation energy  $U$  ( $=U_L+U_H$ ) against the heavy mass  $A_H$ . The well-known minimum at  $A_H \approx 134$  for both nuclei is attributed to the  $[p_{1/2}^p, (g_{7/2}, d_{5/2})^n]_L$  plus  $[g_{9/2}^p, h_{11/2}^n]_H$  subshell closures.

The total energy released,  $E_R$ , agrees reasonably well with the predictions of the mass formulas.<sup>19,20</sup> The predicted kinetic energies  $\frac{1}{2}T$  as a function of the heavy mass  $A_H$  agree with experiments within  $\pm 5$

MeV (the typical experimental errors in the measurements are  $\pm 4$  MeV).

Preliminary work with other fissile nuclei are in progress.<sup>21</sup>

We are thankful to Professor M. K. Pal and Dr. A. K. Sengupta of this Institute for helpful discussions and to Miss S. Chatterjee for partial collaboration in this work. We are thankful to Professor W. Greiner for sending reports of the work of his group.

<sup>20</sup> J. Wing and J. D. Varley, Argonne National Laboratory Report No. ANL-6886, 1964 (unpublished).

<sup>21</sup> R. Sarkar and A. Chatterjee, Phys. Letters **30B**, 313 (1969).

## Complete-Fusion Cross Sections for the Reactions of Heavy Ions with Cu, Ag, Au, and Bi

JOSEPH B. NATOWITZ

*Department of Chemistry and Cyclotron Institute, Texas A&M University, College Station, Texas 77843*

(Received 8 September 1969)

Mica track detectors were used to detect recoil nuclei from the reactions of  $^{12}\text{C}$ ,  $^{16}\text{O}$ , and  $^{20}\text{Ne}$  projectiles with Cu, Ag, Au, and Bi targets. The observed track-length distributions and angular distributions together with detector-threshold information indicate that the observed recoils result from complete fusion of the target and projectile nuclei. The cross section  $\sigma_{\text{CF}}$  for the complete fusion mechanism is found to be well below the total-reaction cross section  $\sigma_R$  at the higher projectile energies. A sharp-cutoff model is employed to extract values of  $J_{\text{crit}}$ , the maximum angular momentum of the compound nuclei formed in complete-fusion reactions. Using those values, complete-fusion cross sections are calculated as a function of the mass of the complete-fusion product for reactions induced by  $^{16}\text{O}$ ,  $^{20}\text{Ne}$ , and  $^{40}\text{Ar}$ . Assuming only first-chance fission, the ratio  $\Gamma_f/\Gamma_n$  has been calculated for the system  $^{197}\text{Au}+^{16}\text{O} \rightarrow ^{213}\text{Fr}^*$ .

### I. INTRODUCTION

THE formation of a compound nucleus by fusion of target and projectile nuclei has long been recognized as a dominant mechanism in heavy-ion-induced nuclear reactions.<sup>1</sup> The high probability of such reactions has made them particularly useful in studies of the properties of highly excited nuclei and in the synthesis of new isotopes and elements.<sup>2</sup> Both of these areas of study can benefit greatly from more specific information concerning the fraction of the total-reaction cross section which is accounted for by complete-fusion reactions. Such information should serve to better characterize the initial conditions for statistical-model evaporation calculations. This should, in turn, serve to further delineate those parameters describing the level density of highly excited nuclei and lead to more reliable predictions of the probability for forming new nuclei. Various approximations to the complete-fusion cross section have been obtained by adding cross sections for individual species obtained by radiochemical techniques.<sup>3,4</sup> The fission fragment angular correlation

experiments of Sikkeland, Haines, and Viola,<sup>5</sup> the emulsion experiments of Pfohl<sup>6</sup> and the track detector experiments of Kowalski, Jodogne, and Miller<sup>7</sup> provide more direct measures of the complete-fusion cross sections. Thomas has recently reviewed heavy-ion reactions and discusses the status of such measurements.<sup>1</sup> It is the purpose of the present paper to report further experimental measurements of the complete-fusion cross sections for heavy ion reactions and to show that the presently available data are consistent with a mass-dependent upper limit to the angular momentum of compound nuclei formed in complete-fusion reactions.

### II. EXPERIMENTAL MEASUREMENTS

The experimental technique employed in this work is similar to that of Ref. 7.

#### A. Irradiations

For the Cu and Ag experiments, thin ( $\sim 160$  to  $500$   $\mu\text{g}/\text{cm}^2$ ) self-supporting targets were prepared by

<sup>5</sup> T. Sikkeland, E. Haines, and V. Viola, Phys. Rev. **125**, 1350 (1962); T. Sikkeland and V. Viola, in *Proceedings of the Third Conference on Reactions between Complex Nuclei, Asilomar, California* (University of California Press, Berkeley, 1963), p. 232; T. Sikkeland, University of California Lawrence Radiation Laboratory Report No. UCRL-181877, 1968 (unpublished).

<sup>6</sup> R. Pfohl, Ann. Phys. (Paris) **1**, 353 (1966).

<sup>7</sup> L. Kowalski, J. C. Jodogne, and J. M. Miller, Phys. Rev. **169**, 894 (1968).

<sup>1</sup> T. D. Thomas, Ann. Rev. Nucl. Sci. **18**, 343 (1968).

<sup>2</sup> G. T. Seaborg, Ann. Rev. Nucl. Sci. **18**, 53 (1968).

<sup>3</sup> J. M. Alexander and G. N. Simonoff, Phys. Rev. **133**, B93 (1964).

<sup>4</sup> R. Bimbot, M. LeFort, and A. Simon, J. Phys. (Paris) **29**, 563 (1968).

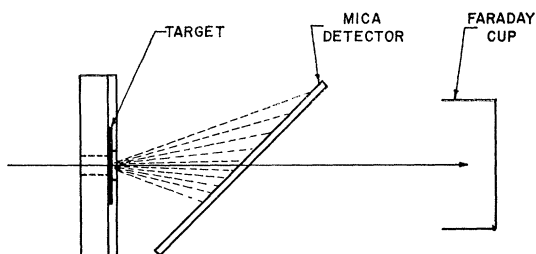


FIG. 1. Experimental geometry. Mica detectors placed in beam at a  $45^\circ$  angle intercept nuclear reaction recoils from thin self-supporting targets mounted on a carbon collimator.

vacuum evaporation. The gold targets ( $\sim 225 \mu\text{g}/\text{cm}^2$ ) were of commercial gold leaf which was 96.4% Au, 2% Ag, and 1.6% Cu. Bi targets ( $\sim 100 \mu\text{g}/\text{cm}^2$ ) were evaporated on a  $200\text{-}\mu\text{g}/\text{cm}^2$  C backing.

The actual experimental geometry is shown in Fig. 1. For an irradiation, the targets were mounted on a carbon collimator in a small vacuum chamber. Two to four centimeters down stream, mica track detectors were mounted in beam tilted at a  $45^\circ$  angle. Energetic nuclei emitted from the target at angles from  $0^\circ$  to  $\sim 45^\circ$  were intercepted by these detectors. Prior to being used, these detectors were annealed for  $\sim 2$  h at  $600^\circ\text{C}$  and etched in room-temperature HF for  $\sim 6$  h.

Irradiations were performed with  $^{12}\text{C}$ ,  $^{16}\text{O}$ , and  $^{20}\text{Ne}$  from the Yale Heavy-Ion Linear Accelerator. Projectile energies lower than  $10.5 \text{ MeV}/\text{amu}$  were obtained by inserting degraders in beam before the final bending magnet. Energies were determined from the range-energy curves of Northcliffe.<sup>8</sup> Typically targets were irradiated for several minutes with beams of 5 to 10 nA as registered by the Faraday cup. Since it was not possible to rely on the Faraday cup for absolute integrated beam under these experimental conditions, the Faraday cup was calibrated at each energy by irradiating Bi and Au targets. Following the etching and scanning procedures outlined in Sec. II B, the total number of fission fragments emitted within  $30^\circ$  to the beam was determined. From the known fission cross sections and fission-fragment angular distributions,<sup>9</sup> the Faraday cup readings were converted to actual integrated beam. This calibration proved to be sensitive to track detector thickness. Since the track detectors used ranged in thickness from 4 to  $14 \text{ mg}/\text{cm}^2$ , the calibration was performed for several different detector thicknesses at each energy. It follows then that all of the cross sections reported in this work are relative to the fission data used for the calibration.

<sup>8</sup> L. C. Northcliffe, Phys. Rev. **120**, 1744 (1960).

<sup>9</sup> T. Sikkeland, Phys. Rev. **135**, B669 (1964); V. E. Viola, T. Thomas, and G. T. Seaborg, *ibid.* **129**, 2710 (1963); G. Gordon, A. E. Larsh, T. Sikkeland, and G. T. Seaborg, *ibid.* **120**, 1341 (1960); H. C. Britt and A. R. Quinton, *ibid.* **120**, 1768 (1960); E. Goldberg, H. L. Reynolds, and D. D. Kerlee, in *Proceedings of the Second Conference on Reactions between Complex Nuclei, Gatlingburg, Tennessee* (John Wiley & Sons, Inc., New York, 1960), p. 230.

## B. Scanning

Following the irradiation, the side of the track detector facing the target was etched for 20 min in room-temperature HF. Etching only that surface prevented the development of a dense area of tracks in the beam spot on the back side of the detector which would have made scanning difficult at the center of the distribution.

The detectors were scanned at  $1250\times$  along the strip determined by the intersection of the track detectors with the horizontal plane containing the beam. Typically we would observe large numbers of well developed, varying length, parallel tracks. The typical length distributions of these tracks are presented in Fig. 2 and will be discussed in more detail below. Often we would also observe small spots ( $\sim 0.5 \mu$  diam). In the region of the beam spot, we also noted some very thin tracks generally not aligned with the larger width tracks which were those being counted and some "bright diamonds" apparently resulting from partial registration of the incident heavy-ion projectiles.<sup>10</sup> These diamonds were a problem only in the  $^{20}\text{Ne}$

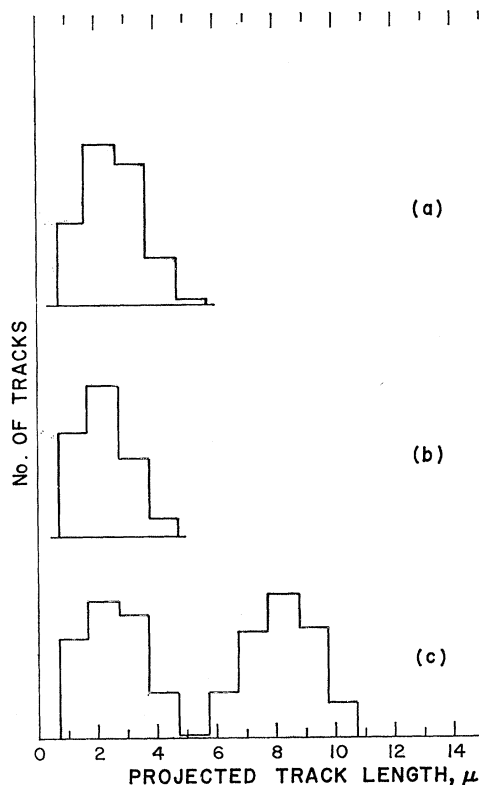


FIG. 2. Track-length distributions for reactions with  $10.5\text{-MeV}/\text{amu}$   $^{16}\text{O}$ . The distributions are for reactions with targets of (a) Cu ( $488 \mu\text{g}/\text{cm}^2$ ), (b) Ag ( $159 \mu\text{g}/\text{cm}^2$ ), (c) Au ( $225 \mu\text{g}/\text{cm}^2$ ). Each distribution represents approximately  $10^3$  tracks.

<sup>10</sup> J. B. Natowitz, J. M. Alexander, and A. Khodai Joopari, Phys. Rev. **169**, 993 (1968).

irradiations where it was necessary to alter the scanning illumination in order to scan the tracks on an intense background of diamonds.

Since it was the purpose of these experiments to determine complete-fusion cross sections, it is necessary to ascertain first that the recoiling product nuclei will leave an etchable track in the detector and that those tracks being counted correspond to complete-fusion events. These points are considered further in this section.

### 1. Registration Thresholds

The registration properties of mica are a function of both mass and energy of the incident ion. Fleischer, Price, and Walker<sup>11</sup> have determined the region of 100% registration. Recent work by Mahony and Alexander<sup>12</sup> serves to further define the registration thresholds. In particular, this latter work indicates that for ions above the mass threshold of mica, 100% registration will occur when the incident energy is  $\geq 0.04$  to 0.05 MeV/amu. The energies of recoils  $E_R$  from complete-fusion reactions may be calculated according to the relationship

$$E_R = A_P A_R E_P / A_{CF}^2. \quad (1)$$

$E_P$  is the laboratory energy of the projectile.  $A_P$  and  $A_R$  are the masses of the projectile and recoil nuclei, respectively.  $A_{CF}$  is the sum of the target and projectile masses. Except for the irradiations of Bi and Au with 126-MeV  $^{12}\text{C}$  and the lower-energy irradiations of Au with  $^{16}\text{O}$ , the complete-fusion recoils produced in these experiments have average energies  $> 0.04$  MeV/amu.

Several radiochemical studies have been performed in which the ranges and range distributions for both complete-fusion and incomplete-fusion reactions have been measured.<sup>13-16</sup> In these studies, incomplete-fusion or transfer reactions are found to decrease in cross section with increasing number of transferred nucleons. Except very near the Coulomb barrier, the ranges of products resulting from a transfer mechanism are much lower than the range of products from complete-fusion reactions. Typically, the average range of complete-fusion products is  $\sim 3$  times that of incomplete-fusion products at the projectile energies employed in the experiments reported in this paper. While particle emission and straggling serve to broaden the range distributions an examination of the cited references indicates that there is in general relatively little overlap between the lowest-range complete-fusion products and the highest-range incomplete-fusion products.

<sup>11</sup> R. L. Fleischer, P. B. Price, and R. M. Walker, *Ann. Rev. Nucl. Sci.* **15**, 1 (1965).

<sup>12</sup> J. Mahony and J. M. Alexander (private communication).

<sup>13</sup> J. M. Alexander and L. Winsberg, *Phys. Rev.* **121**, 529 (1961).

<sup>14</sup> J. B. J. Read, I. Ladenbauer-Bellis, and R. Wolfgang, *Phys. Rev.* **127**, 1722 (1962).

<sup>15</sup> P. D. Croft, J. M. Alexander, and K. Street, *Phys. Rev.* **165**, 1380 (1968).

<sup>16</sup> P. M. Strudler, I. L. Preiss, and R. Wolfgang, *Phys. Rev.* **154**, 1126 (1967).

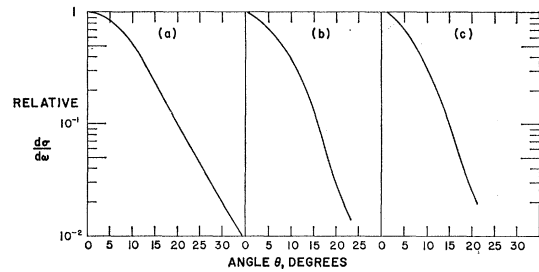


FIG. 3. Angular distribution of tracks for reactions with 10.5 MeV/amu  $^{16}\text{O}$ . The distributions are for reactions with targets of (a) Cu ( $488 \mu\text{g}/\text{cm}^2$ ), (b) Ag ( $159 \mu\text{g}/\text{cm}^2$ ), (c) Au ( $225 \mu\text{g}/\text{cm}^2$ ).

In addition to the 100% registration threshold, the practical scanning threshold must be considered. In this scanning, an event was counted as a complete-fusion event if it were oriented properly in the field, had the appearance of a track, and had a length  $> 0.5 \mu$ . As the angle of entry was  $45^\circ$ , this last requirement is that the track be  $> 0.7 \mu$  long which is  $\sim 200 \mu\text{g}/\text{cm}^2$  of mica (which is equivalent to  $\sim 200 \mu\text{g}/\text{cm}^2$  of Al).

The average ranges of incomplete-fusion products reported in the cited references are  $200\text{--}300\text{-}\mu\text{g}/\text{cm}^2$  Al or roughly equal to the scanning threshold. In addition, the energy threshold of 0.04 to 0.05 MeV/amu implies an unetchable tip to the track left by the recoiling nucleus which is itself  $\sim 300 \mu\text{g}/\text{cm}^2$  or  $1 \mu$ .

It appeared, therefore, that it should be feasible to count tracks resulting from the recoil of complete-fusion reactions in the absence of significant interference from incomplete-fusion reactions. This point was further checked by observation of the length distributions and angular distributions of the observed tracks.

### 2. Track-Length Distributions

Track-length distributions observed in  $^{16}\text{O}$  irradiations at 10.5 MeV/amu are presented in Fig. 2. For irradiations of Cu and Ag, the product track-length distributions appear as a single group peaking at a range close to that expected for complete-fusion reactions. For irradiations of Au, two peaks result corresponding to a shorter group of tracks with a peak length close to that expected for complete-fusion recoils and a peak of greater length corresponding to fission fragments.

### 3. Angular Distributions

In Fig. 3 are presented some representative angular distributions for irradiations with 10.5-MeV/amu  $^{16}\text{O}$ . In each case, we note that those tracks identified with complete-fusion reactions are contained in rather small forward-directed cones. Such an angular distribution argues against significant contributions from transfer reactions or elastic scattering events. The former should have angular distributions which are characteristically broad<sup>15</sup> and would extend well beyond the region scanned.

TABLE I. Complete-fusion cross sections measured in this work.<sup>a</sup>

Projectile	Target	Laboratory		$\sigma_R^b$ (mb)	$\sigma_{CF}/\sigma_R$	
		energy (MeV)	$\sigma_{CF}$ (mb)			
<sup>16</sup> O	Cu	168	653	2080	0.314	
		168	863	2080	0.415	
		136	794	1930	0.411	
		129	912	1900	0.480	
		111	825	1700	0.485	
		97.6	1040	1530	0.680	
		Ag	168	683	2270	0.301
			168	670	2270	0.295
			168	646	2270	0.285
			168	768	2270	0.338
	136		782	1960	0.399	
	130		900	1890	0.476	
	114		865	1660	0.521	
	111		999	1600	0.624	
	97.6		1190	1390	0.856	
	<sup>197</sup> Au <sup>c</sup>		168	116	2500	0.686
		168	56	2500	0.662	
		168	113	2500	0.685	
		136	75.8	2000	0.673	
		136	87.2	2000	0.679	
129		107	1850	0.696		
111		422	1350	0.883		
99.5		360	950	0.937		
97.6		416	880	0.981		
<sup>209</sup> Bi <sup>c</sup>		168	159	2400	0.691	
<sup>20</sup> Ne	Cu	117	118	1390	0.927	
		210	532	2170	0.245	
	Ag	169	640	1970	0.325	
		210	672	2340	0.287	
	<sup>197</sup> Au <sup>c</sup>	173	868	2070	0.419	
		210	63.4	2400	...	
<sup>209</sup> Bi <sup>c</sup>	210	81	2540	0.574		
<sup>12</sup> C	Cu	126	536	1980	0.271	
		Ag	126	906	2140	0.423
	<sup>197</sup> Au <sup>c</sup>	126	104	2200	0.638	
	<sup>209</sup> Bi <sup>c</sup>	126	139	2260	0.672	

<sup>a</sup> Estimated errors are  $\pm 20\%$  for Cu, Ag, Bi and  $\pm 30\%$  for Au.

<sup>b</sup> Total-reaction cross sections for reactions with Cu, Ag, and Au are from Ref. 18. For Bi, Eq. (2) was used to calculate the total-reaction cross sections.

<sup>c</sup> The cross sections for Au and Bi irradiations do not include the fission cross section. The fission cross section has been included in the calculation of  $\sigma_{CF}/\sigma_R$ .

In elastic scattering, the cross section for scattering of heavy-target nuclei is highest for scattering at large angles to the beam and decreases rapidly for forward scattering. Thus, if significant numbers of such events were being detected in these experiments, the number of such tracks would increase with increasing angle in contrast to the experimental observation. In addition, elastically scattered heavy nuclei directed at small angles to the beam would leave much longer tracks than those from complete-fusion events. That such events do not make a significant contribution to the tracks which we are counting is entirely consistent with the observed

cutoff of Coulomb scattering at impact parameters corresponding to the nuclear radii.<sup>17</sup>

On the basis of the arguments presented in this section, it appears that the tracks being counted in these experiments correspond to the registration of complete-fusion events with essentially 100% efficiency. It is probable that a small fraction of the complete-fusion events are not being detected and further that a small fraction of incomplete-fusion events are being detected. To some extent these effects should compensate.

### III. COMPLETE-FUSION CROSS SECTIONS

The total number of complete-fusion events was determined by numerical integration of the measured angular distributions. Complete-fusion cross sections  $\sigma_{CF}$  were then calculated.

The overriding consideration in determining the errors in these experiments are the errors inherent in the scanning. It is estimated that the cross sections for irradiation of Cu, Ag, and Bi are accurate to  $\pm 20\%$ . For Au,  $\pm 30\%$  is estimated since significant corrections were made for the Ag and Cu impurities.

In Table I, the complete-fusion cross sections determined in the present work are presented. For Au and Bi, the cross sections measured are for complete-fusion reactions in which fission does not occur. To obtain the total complete-fusion cross section, the fission cross sections reported in the literature<sup>9</sup> have been added as indicated. Angular correlation measurements of the fission fragments<sup>9</sup> indicate that for Bi and lighter targets, incomplete-fusion reactions with <sup>12</sup>C and <sup>16</sup>O contribute not more than 1% to the fission cross sections. In reactions with <sup>20</sup>Ne, the incomplete-fusion contribution is  $\sim 7\%$  for Au targets and  $\sim 10\%$  for Bi targets.

In Table I, the values of  $\sigma_{CF}/\sigma_R$  for heavy-ion irradiations of Cu, Ag, and Au were taken from the total-reaction cross sections  $\sigma_R$  calculated by Thomas.<sup>18</sup> In Ref. 1, these calculations are shown to be in good agreement with the limited experimental data on total-reaction cross sections. For Bi, the total-reaction cross sections were calculated according to the expression

$$\sigma_R = \pi R^2 (1 - V/E_{c.m.}), \quad (2)$$

where  $R$  is the sum of the target and projectile radii,  $V$  is the Coulomb barrier, and  $E_{c.m.}$  is the energy in the center of mass. When an interaction radius parameter  $r_0 = 1.46 F$  and a Coulomb barrier assuming tangent spheres are used in the above expression, the calculated cross sections agree to  $\pm 5\%$  with those of Ref. 18. Thus Eq. (2) should be a useful formula for approximating total-reaction cross sections for other systems.

In Figs. 4-6, the measured cross sections for complete fusion of Cu, Ag, and Au with <sup>16</sup>O projectiles are

<sup>17</sup> J. A. McIntyre, S. D. Baker, and T. L. Watts, Phys. Rev. **116**, 1212 (1959).

<sup>18</sup> T. D. Thomas, Phys. Rev. **116**, 703 (1959).

plotted. As found in previous work and evidenced in Table I, the discrepancy between complete-fusion cross sections and the total-reaction cross sections increases with increasing bombardment energy and  $\sigma_{CF}$  is well below the total-reaction cross section at 10.5 MeV/amu.

The data reported here may most directly be compared with the data of Refs. 4, 6, and 7. There appear to be no discrepancies between the magnitudes of the complete-fusion cross sections of this work and those of the other workers.

#### IV. INTERPRETATION

Various calculations have suggested that complete-fusion cross sections might be significantly less than total-reaction cross sections when heavy ions are

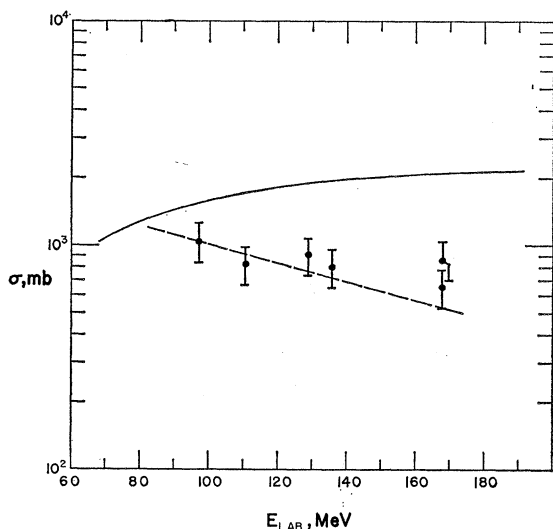


FIG. 4. Complete-fusion cross sections for the reactions of  $^{160}$  with Cu. The experimental data is indicated by the solid points and error bars. The solid line is the total-reaction cross section from Ref. 18. The dashed line shows the trend of  $\sigma_{CF}$  calculated according to the model of Kalinkin and Petkov with the parameters indicated in the text.

employed as projectiles.<sup>19-21</sup> These calculations, based on a liquid-drop model, indicate that the nuclear shape is distorted with increasing angular momentum until a critical angular momentum is reached for which the nuclear shape is no longer stable. Thus, above this critical angular momentum, complete fusion will not occur.

A relatively simple approach of this type has been followed by Kalinkin and Petkov<sup>21</sup> who have assumed that complete fusion leads to an ellipsoidal-shaped

<sup>19</sup> R. Beringer and W. J. Knox, Phys. Rev. **121**, 1195 (1961).

<sup>20</sup> S. Cohen, F. Plasil, and W. J. Swiatecki, in *Proceedings of the Third Conference on Reactions between Complex Nuclei, Asilomar, California* (University of California Press, Berkeley, 1963), p. 325.

<sup>21</sup> B. N. Kalinkin and I. Z. Petkov, Acta Phys. Polon. **25**, 265 (1964); University of California Lawrence Radiation Laboratory Report No. UCRL Trans-1151, 1964 (unpublished).

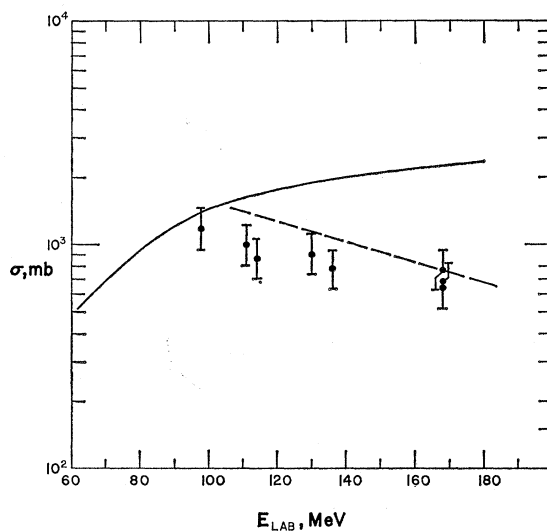


FIG. 5. Complete-fusion cross sections for the reactions of  $^{160}$  with Ag. The experimental data is indicated by the solid points and error bars. The solid line is the total-reaction cross section from Ref. 18. The dashed line shows the trend of  $\sigma_{CF}$  calculated according to the model of Kalinkin and Petkov with the parameters indicated in the text.

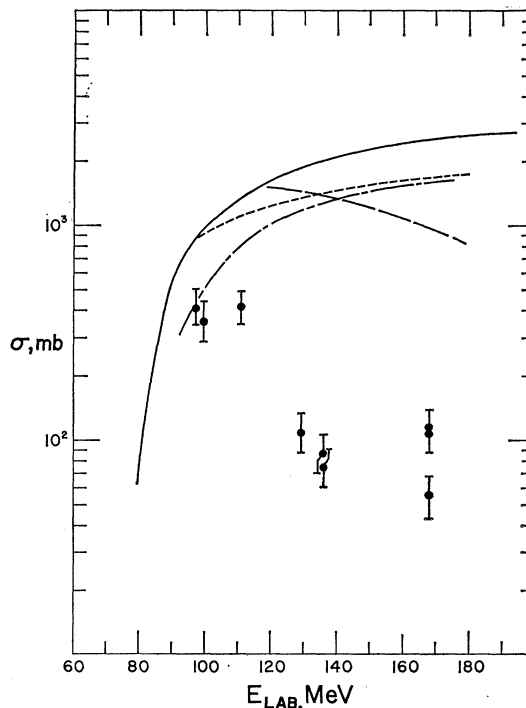


FIG. 6. Complete fusion cross sections for the reactions of  $^{160}$  with Au. The solid points with error bars indicate the cross section for complete fusion which is not followed by fission. The solid line is the calculated total reaction cross section from Ref. 18. The alternating long and short dashes show the fission excitation function. The short dashes indicate the total complete-fusion cross section including fission. The long dashes indicate the complete-fusion cross sections calculated according to the method of Kalinkin and Petkov with the parameters indicated in the text.

nucleus. Taking  $R$  as the radius of a sphere with volume equal to the sum of the volumes of the colliding nuclei, the major semiaxis of the ellipse is assumed as

$$a = R + [A_p / (A_t + A_p)] R(l, E), \quad (3)$$

where  $R(l, E)$ , a function of orbital angular momentum and projectile energy, is the distance of closest approach of the nuclei. The eccentricity  $\epsilon$  is defined as

$$\epsilon = (1 - b^2/a^2)^{1/2}, \quad (4)$$

where  $b$  is the semiminor axis of the ellipse. A value is then derived for  $L_{\text{crit}}$ , the maximum orbital angular momentum of the projectile which will lead to a stable system,

$$L_{\text{crit}}^2 = \frac{2Ia}{\hbar^2} \frac{2 - \epsilon^2}{1 + \epsilon^2} \left[ \pi S b \{ (1 - \epsilon^2)^{1/2} + \epsilon^{-1} \arcsin \epsilon \} \right. \\ \left. + 3 \frac{1 - \epsilon^2}{\epsilon^2} \{ (1 - \epsilon^2)^{1/2} - \epsilon^{-1} \arcsin \epsilon \} \right] \\ + 0.9 \frac{(Z_{\text{CF}} e)^2}{a^2 \epsilon^2} \left( 1 - \frac{3 - \epsilon^2}{6\epsilon} \ln \frac{1 + \epsilon}{1 - \epsilon} \right). \quad (5)$$

In this expression,  $I$  is the moment of inertia taken here as  $I_{\text{rigid}}$ .

$$I_{\text{rigid}} = \frac{1}{5} A_{\text{CF}} M_a^2 (2 - \epsilon^2), \quad (6)$$

where  $M$  is the nucleon mass.  $S$  is the surface-tension parameter taken here as 0.95 MeV/F<sup>2</sup> and  $Z_{\text{CF}} e$  is the nuclear charge of the compound nucleus.

$R(l, E)$  is also a root of the equation

$$E_{\text{c.m.}} - V_q(R) - V_N(R) - (\hbar^2/2\mu)(L^2/R^2) = 0, \quad (7)$$

where  $V_q$  is the Coulomb potential and  $V_N$  is the Woods-Saxon potential.

The Coulomb potential used was that allowing for a nonuniform charge distribution characterized by a parameter  $n$ , taken as 10 in this model.<sup>22</sup> The Woods-Saxon potential is

$$V_N(R) = -V_0 \{ 1 + \exp[(R - R_0)/a_0] \}^{-1}. \quad (8)$$

For these calculations,  $V_0 = 40$  MeV,  $a_0 = 0.45$ ,  $R_0 = r_0(A_p^{1/3} + A_t^{1/3})$ , and  $r_0 = 1.22$  F. If Eqs. (5) and (7) are solved simultaneously, the value of  $L_{\text{crit}}$  at a particular projectile energy can be obtained. When  $L_{\text{crit}}$  is less than  $L_{\text{max}}$ , the maximum possible angular momentum of the system, the complete-fusion cross section may be calculated according to the expression

$$\sigma_{\text{CF}}(E) = \pi \hbar^2 L_{\text{crit}}^2 / 2\mu E_{\text{c.m.}} \quad (9)$$

In Figs. 4-6, the dashed lines correspond to calculations of  $\sigma_{\text{CF}}$  with the Kalinkin model. In addition to the other parameters  $I/I_{\text{rigid}}$  was taken as equal to 1.0. The cross sections calculated in this manner are in fair

agreement with the experiments at lower masses but deviate considerably at higher masses. The magnitude of the calculations is quite sensitive to the choice of  $r_0$ ,  $I/I_{\text{rigid}}$ , and  $S$  parameters. In contrast, the shape of the calculated  $\sigma_{\text{CF}}$  in the region where  $\sigma_{\text{CF}} < \sigma_R$  is quite insensitive to the parameter choices.

### A. Empirical Angular Momentum Limit

The concept of a limiting angular momentum can be further explored by employing a simple sharp-cutoff model to extract values of the critical angular momentum for compound nuclei formed in complete-fusion reactions. For this purpose, targets and projectiles of intrinsic spin = 0 are assumed, i.e.,  $J_{\text{max}} = L_{\text{max}}$ .

The nature of the assumptions of this model is indicated in Fig. 7. It is assumed that if all of the reactions were of the complete-fusion type, the angular momentum spectrum of the compound nuclei would be well approximated by a distribution function  $P(J)$  such that

$$P(J) dJ = (2J/J_{\text{max}}^2) dJ, \quad J < J_{\text{max}}$$

$$P(J) dJ = 0, \quad J > J_{\text{max}}$$

and

$$J_{\text{max}}^2 = 2\mu(E_{\text{cm}} - V)R^2/\hbar^2. \quad (10)$$

Since incomplete-fusion reactions are expected to occur at the nuclear surface, the assumption is made that there is a value  $J_{\text{crit}} < J_{\text{max}}$  such that the angular momentum distribution of the nuclei formed in complete-fusion reactions is cut off at  $J_{\text{crit}}$ . It follows then that

$$J_{\text{crit}} = (\sigma_{\text{CF}}/\sigma_R)^{1/2} J_{\text{max}}. \quad (11)$$

Using data from the literature<sup>3,5,7,23</sup> together with the cross sections reported in this work, values of  $\sigma_{\text{CF}}/\sigma_R$  have been calculated. For this purpose, the total-reaction cross section was taken from Ref. 18 or calculated with Eq. (2). The data taken from Refs. 3 and 23 actually correspond to complete-fusion reactions following which only neutrons and  $\gamma$  rays are emitted.

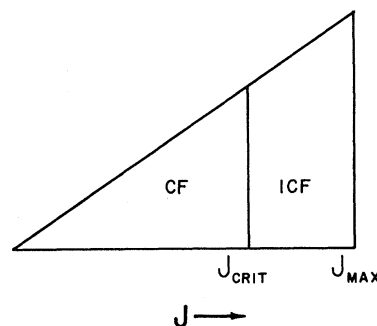


FIG. 7. Sharp-cutoff model. The angular momentum distribution for compound nuclei resulting from complete-fusion reactions is taken as triangular with a maximum at  $J_{\text{crit}}$ .

<sup>22</sup> D. L. Hill and K. W. Ford, Phys. Rev. **94**, 1617 (1954).

<sup>23</sup> J. B. Natowitz and J. M. Alexander, Phys. Rev. **188**, 1734 (1969).

In the heavier elements, such reactions might be expected to account for the bulk of the compound-nucleus cross section. It is of interest to compare values of  $J_{\text{crit}}$  derived from those measurements with values derived from measurements of the complete-fusion cross section.

In the lower portion of Fig. 8,  $\sigma_{\text{CF}}/\sigma_R$  is plotted against  $A_{\text{CF}}$  for reactions leading to compound nuclei with excitation energies from 75 to 125 MeV. The type of projectile and the actual excitation energy are indicated by the choice of symbols as explained in the figure caption. The tendency of  $\sigma_{\text{CF}}/\sigma_R$  to decrease with increasing excitation energy and projectile mass is easily observed in this figure. From each of those measurements, the quantity  $J_{\text{crit}}$  has been extracted in the method described. In the upper portion of Fig. 8,  $J_{\text{crit}}$  is plotted as a function of  $A_{\text{CF}}$ . The extraction of values of  $J_{\text{crit}}$  from complete-fusion cross-section measurements for reactions with  $^{16}\text{O}$  and heavier projectiles appears to lead to values of  $J_{\text{crit}}$  which are the same within experimental error. Values derived from reactions with  $^{12}\text{C}$  fall about 20% below the other data. The  $J_{\text{crit}}$  values derived from the  $(xn)$  cross-section measurements of Refs. 3 and 23 appear consistent with the other data, although probably lower than would be obtained from complete-fusion cross-section measurements.

The dotted line in the upper portion of Fig. 8 is presented for comparison and represents the calculated

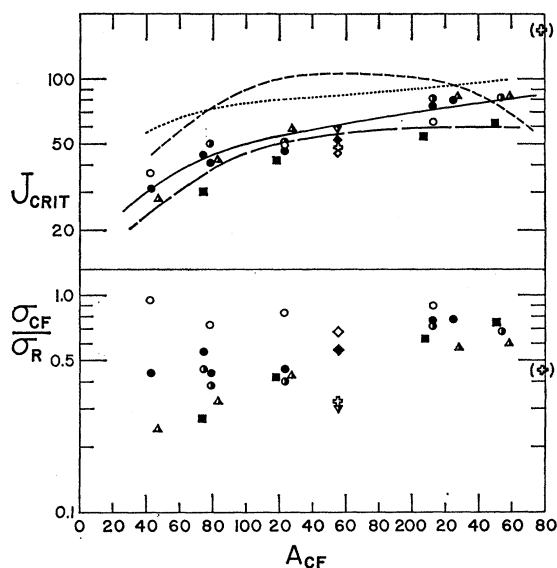


FIG. 8.  $\sigma_{\text{CF}}/\sigma_R$  and  $J_{\text{crit}}$  as a function of mass of the compound system. Symbols are as follows:  $^{12}\text{C}$ ,  $\blacksquare$ ;  $^{14}\text{N}$ ,  $\blacklozenge$ ;  $^{16}\text{O}$ ,  $\bullet$ ;  $^{20}\text{Ne}$ ,  $\blacktriangle$ ;  $^{22}\text{Ne}$ ,  $\blacktriangledown$ ;  $^{40}\text{Ar}$ ,  $\blackplus$ . Ar points at  $A_{\text{CF}}=278$  are for experiments with 415-MeV  $^{40}\text{Ar}$ . Other symbols indicate excitation energy; open—75 MeV, solid—100 MeV, composite—125 MeV. Solid line indicates trend of data exclusive of  $^{12}\text{C}$  data and values obtained from  $\sigma(xn)/\sigma_R$  data. Dotted curve indicates calculated  $J_{\text{max}}$  for 10.5-MeV/amu  $^{16}\text{O}$ . Long dashes represent a Kalinkin-Petkov calculation of  $J_{\text{crit}}$  with parameters indicated in text. Short dashes indicate  $J_{\text{crit}}$  from calculations of Ref. 20.

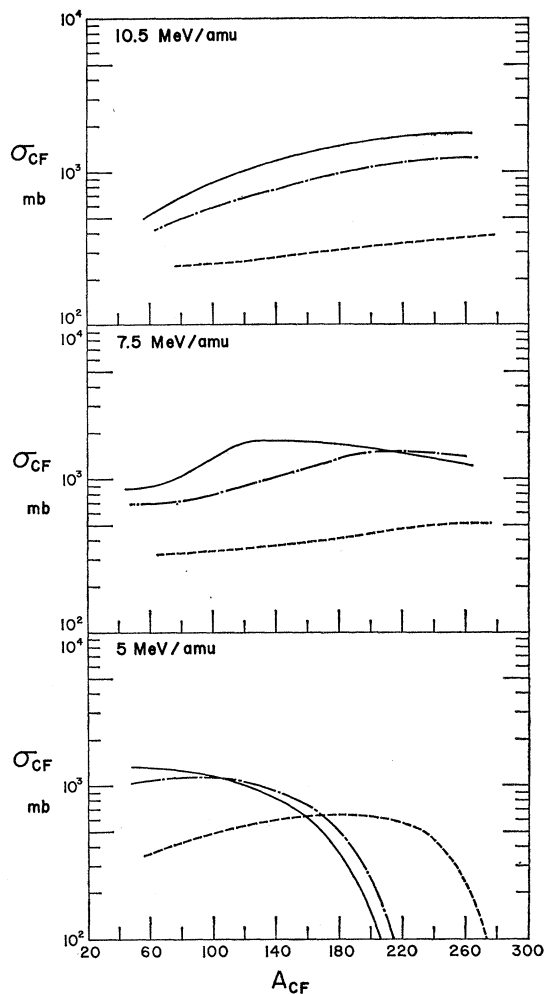


FIG. 9. Calculated complete-fusion cross sections. Values of  $J_{\text{crit}}$  taken from the solid curve of Fig. 8 have been used in Eq. (9) to calculate  $\sigma_{\text{CF}}$  as a function of mass for 5-, 7.5- and 10.5-MeV/amu projectiles,  $^{16}\text{O}$ —,  $^{20}\text{Ne}$ —,  $^{40}\text{Ar}$ —.

values<sup>18</sup> of  $J_{\text{max}}$  for reactions with 160-MeV  $^{16}\text{O}$ . Calculations of  $J_{\text{crit}}$  with the Kalinkin model of 100-MeV excitation energy are also presented in Fig. 8. The calculations were made using the same parameters as were used for the  $\sigma_{\text{CF}}$  calculations of Figs. 4–6. Varying these parameters could somewhat improve the agreement with the experimental data at the high masses but results in poorer fits to the available excitation functions.

The short-dashed line of Fig. 8, taken from Fig. 5 of Ref. 1 shows the behavior of  $J_{\text{crit}}$  indicated by the calculations of Cohen, Plasil, and Swiatecki for nuclei near the line of stability. This latter calculation allowed for considerably more variation of nuclear shape than the model used by Kalinkin. It appears to considerably overestimate the critical angular momentum at intermediate masses.

It will be noted that the value of  $J_{\text{crit}}$  derived from the fission-fragment angular correlation experiments<sup>5</sup>

TABLE II.  $\Gamma_f/\Gamma_n$  for the system  $^{197}\text{Au}+^{16}\text{O}\rightarrow^{213}\text{Fr}^*$  calculated assuming only first-chance fission.

Excitation energy (MeV)	$\Gamma_f/\Gamma_n$
60.1	1.33
69.4	1.89
78.6	5.55
87.9	11.1
97.0	15.9
106.0	18.5
115.0	20.0

for the reaction of 10.5-MeV/amu  $^{40}\text{Ar}$  with  $^{238}\text{U}$  is about twice that derived from other experiments in this region. No angular distributions were measured in those experiments and it may be that the geometry employed (one detector fixed at  $90^\circ$  to the beam) leads to overestimates of the complete-fusion cross section. If this is not the case, there would appear to be a significant change in  $J_{\text{crit}}$  with either projectile mass (also suggested by the  $^{12}\text{C}$  reactions) or excitation energy. More data for heavier-mass projectiles is clearly required.

## V. DISCUSSION

From the success of the simple model in correlating the data on  $\sigma_{\text{CF}}/\sigma_R$ , it appears that the angular momentum distribution characterized by a cutoff at  $J_{\text{crit}}$  is a reasonable approximation to the initial distribution of compound nuclei formed in complete-fusion reactions.

Recent statistical model evaporation calculations in which angular momentum effects are considered predict the enhancement of  $\alpha$ -particle emission at high angular momentum.<sup>24</sup> For example at 20-MeV excitation in  $^{153}\text{Dy}$ ,  $\alpha$ -particle emission is predicted to increase sharply for states of angular momentum  $\gtrsim 40\hbar$ . Since this is below the  $\sim 60\hbar$  maximum angular momentum suggested by Fig. 8 for this mass region, such effects would still be expected but reduced by the more limited population of states with angular momentum greater than  $40\hbar$ . The values of  $J_{\text{crit}}$  derived from  $(xn)$  cross-section measurements do seem to be somewhat lower than might result from measurements of the complete-fusion cross sections. Further measurements of complete-fusion cross sections are contemplated in the intermediate mass region.

### A. Calculated Complete-Fusion Cross Sections

If the value of  $J_{\text{crit}}$  is assumed to be independent of excitation energy and projectile mass,<sup>19,20</sup> complete-

<sup>24</sup> J. R. Grover and J. Gilat, Phys. Rev. **157**, 802 (1967).

fusion cross sections may be calculated for various heavy-ion projectiles incident on any chosen target. In Fig. 9, the results of such a calculation for  $^{16}\text{O}$ ,  $^{20}\text{Ne}$ , and  $^{40}\text{Ar}$  projectiles at 5, 7.5, and 10.5 MeV/amu are indicated. The cross sections were calculated according to a sharp-cutoff model using Eq. (9).

The figures should be useful for estimating  $CF$  cross sections to  $\pm 20\%$ .

## VI. $\Gamma_f/\Gamma_n$ FOR $^{197}\text{Au}(^{16}\text{O}, f)$

In the region of masses and excitation energies where fission is an important mode of nuclear deexcitation, knowledge of the partial widths for fission decay is very useful. By making two assumptions, it is possible to derive values of the ratio  $\Gamma_f/\Gamma_n$  for the nucleus  $^{213}\text{Fr}^*$  produced in the complete-fusion reactions of  $^{16}\text{O}$  with  $^{197}\text{Au}$ . The assumptions are:

- (1) Only first-chance fission occurs.
- (2) The nonfission complete-fusion cross sections determined in this work result from only  $xn$  reactions.

With these assumptions, the ratio  $\Gamma_f/\Gamma_n$  has the simple form

$$\Gamma_f/\Gamma_n = [(\sigma_{\text{CF}}/\sigma_{\text{F}}) - 1]^{-1}. \quad (12)$$

In Table II, the values of  $\Gamma_f/\Gamma_n$  calculated from Eq. (12) at various excitation energies are tabulated.

## VII. SUMMARY

The data of this paper combined with other data from the literature support the concept of a mass-dependent limit to the angular momentum of compound nuclei formed in heavy-ion reactions. It has been assumed here that this limit is independent of excitation energy and projectile type. Little evidence is available on this latter point and experiments with heavier projectiles such as  $^{40}\text{Ar}$  would be of considerable value in clarifying this point.

## ACKNOWLEDGMENTS

The author wishes to thank E. Vezey for his help in preparing the thin targets; the staff of the Yale Hilac for their courtesy and assistance during the irradiations; and Mrs. Ona Pridgeon for a conscientious job of scanning the numerous mica detectors. Conversations with Dr. J. Alexander, Dr. J. Mahony, Dr. J. Miller, Dr. L. Kowalski, and Dr. J. Jodogne were particularly helpful. In the early stages, this work was supported by a grant from the Research Council of Texas A & M University. The latter portion of the work was supported by the U. S. Atomic Energy Commission under Contract No. AT-(40-1)-3924.